Flame Height Behavior of Merging Fire Whirls From Multiple Fire Sources

Watanabe N.[1,] *, Sugawa O.[2], Kamiya K.[2]

[1] *Graduate School of Suwa University of Science, Engineering and Management and Electrical Engineering, Chino, Nagano, Japan*

[2] *Suwa University of Science, Department of Mechanical and Electrical Engineering, Chino, Nagano, Japan*

**Corresponding author's email: gh17702@ed.sus.ac.jp*

ABSTRACT

Fires in booths or kiosks on the bottom floor of an atrium space lead to fire spreading to the booths and kiosks one after another, resulting in multiple flame sources and/or flame merging. The airflow in the atrium will create fire whirls from multiple burning locations. Whether the merging of fire whirls in the atrium will present an unacceptable fire hazard has not been adequately studied. We report the results obtained from an examination of flame height behavior as multiple fire whirls merged in small-scale fire tests. The flame behavior determined from the experiments was compared with McCaffrey's model, which divides the temperatures and upward flow of the flame center line into three regions of continuous flame, intermittent flame, and buoyancy plume from a pool fire or a sand gas burner. The strong and stable merging fire whirl expanded the continuous flame region, as determined by comparing the temperature attenuation on the center line with that of McCaffrey's model. As to the contribution to changes in flame height, the distance between fire sources is more dominant than the entrained air amount from air inlets. Our results provide useful information for determining the quantification of the parameter of flame height associated with the fire whirls for merging multiple flames.

KEYWORDS: Merging fire whirl, flame height, multiple fire sources, air inlet.

NOMENCLATURE

D	diameter of fire source (mm)
L	merging fire whirl height for S/D = 0 (mm)
L_m	merging fire whirl height (mm)
n	number of fire sources (-)
$\dot{q}$	heat release rate (kW)
S	distance between fire sources (mm)
ΔT	temperature rise along center axis of fire sources (K)
v	upward flow velocity (m/s)
z_b	bi-directional tube height (mm)
z_t	thermocouple height (mm)

Greek

α_1	coefficient in Eq. (2)
α_2	coefficient in Eq. (2)

INTRODUCTION

In large-scale commercial facilities, enclosed atriums are designed to provide open and spacious vertical areas and form a remarkably pleasant space for persons in the building. In the large space of the atrium, a temperature difference tends to occur in the vertical direction and heat pockets form at its top. Thus, air flows from the bottom toward the top through the entrances and openings by a

Proceedings of the Ninth International Seminar on Fire and Explosion Hazards (ISFEH9), pp. 652-661
Edited by Snegirev A., Liu N.A., Tamanini F., Bradley D., Molkov V., and Chaumeix N.
Published by St. Petersburg Polytechnic University Press
ISBN: 978-5-7422-6496-5 DOI: 10.18720/spbpu/2/k19-59

combination of natural and mechanical ventilation to reduce the heat pockets [1, 2]. This airflow provides a crosswind and upward flow to flames during atrium fires [3].

The bottom floor of an atrium space is sometimes used as an event or exhibition venue. The booths and kiosks in an event or exhibition are designed and constructed entirely of flameproof plywoods, curtains, and accessories to prevent the spread of fire and smoke. Generally, because the goods, exhibits, and fixtures used in such events are not flameproof, an increase in the amounts of those items will increase the potential fire hazard. A fire in one such booth or kiosk spreads to other booths and kiosks one after another due to the ample oxygen present in the large interior of the atrium, thus creating multiple flames. When air entrainment is restrained by another nearby flame or flames, flame merging and extension occurs. Furthermore, these flames can grow into a fire whirl due to the upward airflow in the atrium. Numerous experimental and theoretical studies have been carried out on the behavior of fire whirls [4–12]; however, there has been insufficient study of fire whirl merging behavior and how it is affected by changing the spacing between fire sources.

The flame behaviors of merging multiple fires can be different from that of a single fire because adjacent fires interact [13–16]. Thomas et al. studied the height of merged flames from two square fire sources [14]. One of the authors further studied the effects of fire spacing on the merging flame height of multiple fire sources [15]. They developed an empirical model for flame height estimation for the flames from three or four circular pool fires in a symmetrical arrangement. This empirical model is also very important for the interpretation of the merging flame height of multiple fire whirls. Dermer et al. studied methods to determine parameters for conditions that generate wall-free non-stationary fire whirls from multiple fire sources caused by the axisymmetric flame's instability [16]. This study shows that the height of a fire whirl is determined by the number and spacing of fire sources.

We focused on the fire whirls formed from the merger of multiple flame sources, as in an atrium fire. Then, we experimentally investigated the variations in flame height behavior due to the spacing of the fire sources [17]. A fixed-frame tubular device was used in a series of small-scale fire tests to study flame merging and fire whirl formation. The flame behavior determined from experiments was compared with McCaffrey's model, which divides the temperatures and upward flow velocities of the flame center line into three regions of continuous flame, intermittent flame, and buoyancy plume from a pool fire or a sand gas burner [18]. Our results provide useful information for quantifying the parameters of the flame height associated with flames from multiple sources merging into fire whirls.

EXPERIMENT

The tubular device used to observe the merging of fire whirls was fixed-frame, had a cross-section shaped like a hexa-decagon, and had guide plates made from 16 narrow boards, as shown in Fig. 1. The guide plates were angled to form vertical, narrow tilted openings at equal distances. These openings formed the air inlets that imparted a balanced swirling flow and promoted the merging of multiple fire sources. Five contiguous guide plates on the front side of the tubular device were clear and colorless polycarbonate, and the remaining 11 guide plates on the rear side were medium-density fiberboard. The clear boards were used for flame observation. All boards were rectangular and measured 100 mm × 900 mm × 4 mm. We set the distance R of the center of the tubular device from the center of each guide plate to 253 mm and set the angle of the air inlets to 10 degrees. In a previous study, the authors confirmed that a guide plate angle of 10 degrees was most effective for producing a strong and stable merging fire whirl [17].

The fire sources were six pans set on the bottom board of the tubular device along the circumference of a circle of radius r from the center of the bottom board, as shown in Fig. 2. These pans had an inside diameter *D* of 38 mm, depth of 20 mm, and wall thickness of 0.1 mm. Distance *S* between fire sources was calculated from the value of *r*. The bottom board was made of calcium silicate and placed on an electronic balance with a precision of 0.01 g. The mass loss of the burning 2-propanol was measured with the electronic balance at intervals of 1 second, and the mass loss rate was calculated from this result. The mass loss rate was smoothed by a moving average, and the time width of the steady state, where the mass loss rate is largely independent of time, was investigated. In the moving average, 7 seconds, that is, 7 points, were used. An arbitrary 90-second period in the time width of the steady state of the mass loss rate was selected. Then, the heat release rate was calculated by multiplying the measured mass loss value of this period with the effective heat of combustion of 2-propanol, and we obtained average, minimum, and maximum values. The effective heat of combustion for 2-propanol was 30.46 kJ/g. The total time of 2-propanol combustion in all pans did not exceed 5 seconds. The bottom plate resting on the electronic balance was not in contact with the 16 guide plates.

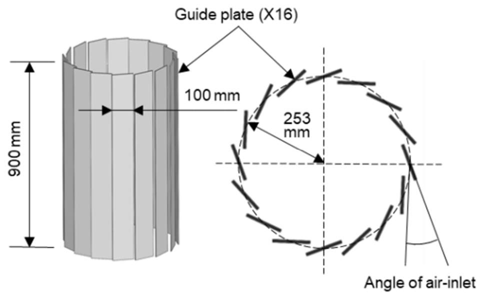

Fig. 1. Schematic for the fire tubular device.

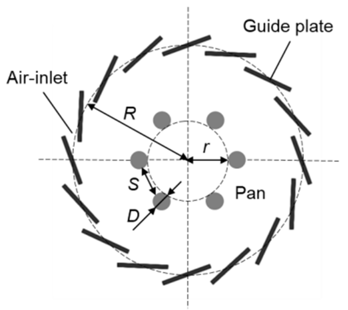

Fig. 2. Location of six fire sources on the bottom board of the tubular device. *D* is the diameter of fire source (mm), *r* is the distance from the tubular device center to a fire source (mm), *R* is the distance from the center of the tubular device to the center of a guide plate (mm), *S* is the distance between fire sources (mm).

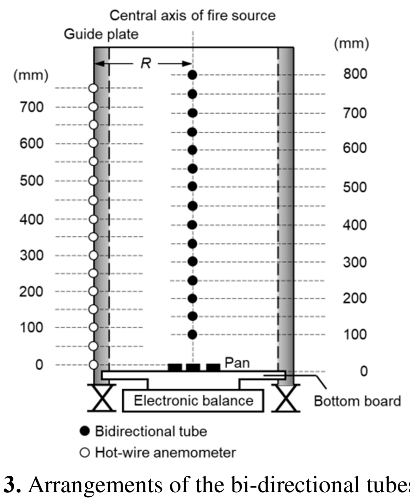

Fig. 3. Arrangements of the bi-directional tubes and hot-wire anemometers in the tubular device.

The temperature profile was measured in the vertical direction in intervals of 50 mm from the top edge of the pans to a height of 1,200 mm by a tree of K-type thermocouples with a diameter of 0.5 mm, and the temperature was recorded at intervals of 1 second. The thermocouple tree was set along the central axis of the tubular device. Figure 3 shows arrangements of the bi-directional flow tubes and hot-wire anemometers in the tubular device. The bi-directional tubes were set along the central axis of the fire source to obtain the upward velocity of the vertical flow and were arranged in the vertical direction at 50-mm intervals from 100 mm above the bottom board to a height of 750 mm. The upward velocity was calculated from the temperature and amplified output of a differential pressure transducer (Validyne, DP103-10-N-3-S-4-D) connected to the bi-directional tubes. The temperature was obtained with K-type thermocouples attached to the bi-directional tubes. The profiles of the temperature and amplifier transducer output were recorded at intervals of 1 second. The airflow velocity in the horizontal direction at the air inlet was measured with hot-wire anemometers (Testo, 435-4). The hot-wire anemometers were arranged in the vertical direction in intervals of 50 mm from the top edge of the pans to a height of 800 mm and placed at distance *R* in one air inlet. Additionally, a video camera was placed outside the clear guide plates of the tubular device to record the experiments at 50 frames per second to determine the flame shape and height.

RESULTS AND DISCUSSION

Heat release rate and flame structure

Figure 4 shows the relation between the dimensionless distance between fire sources S/D and the heat release rate obtained by the six fire sources. S/D is the ratio of the distance between fire sources S and the fire source diameter D. As shown in Fig. 4, the maximum average heat release rate was observed for combustion of $S/D = 0$, and it decreased with increasing S/D. In the range of $0 \leq S/D \leq 0.08$, the burning process decreased significantly with increasing S/D. In addition, the difference between the maximum and minimum values of the flame height was large for $S/D > 0.16$; that is, the fluctuations in flame height were large. We believe that this variation is affected by the distance between the pans and the guide plates.

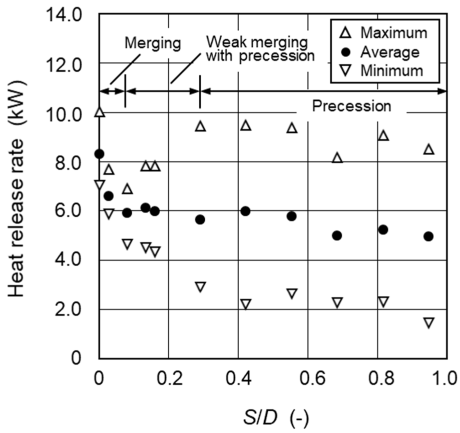

Fig. 4. Variation of heat release rate compared to ratio of distance between fire source *S* and pan diameter *D*.

Figure 5 shows the states of the fire in regions where the burning can be inferred to be in a steady state, as indicated by the heat release rate. A merging fire whirl was observed in the range $0 \leq S/D \leq 0.29$ in Fig. 5. The initial flame merger for these values of S/D tended to begin near the flame base and then extend toward the guide plates; it had a precession relative to the precession of the central axis of the fire source. The inclined merging initial flame indicated that the flow field lost axial symmetry. Additionally, in the range of $0 \leq S/D \leq 0.08$, the unstable merging flame with a weak swirl and precession underwent a transition to become strongly rotating and erect at a steady state. In the range of $0.13 \leq S/D \leq 0.29$, though an unstable flame with weak swirl and precession was observed, it did not undergo a transition to a strongly rotating steady state; rather, a weak merging fire whirl with precession was observed. In addition, while swirl flows with precession were evident in the flames, a merging fire whirl was not formed in the range of $0.42 \leq S/D \leq 0.95$. Although there is almost no difference in the value of the heat release rate, comparison of $0.13 \leq S/D \leq 0.29$ with

$0.42 \leq S/D \leq 0.95$ showed that the flame structure changes. The flame structure in the range $0 \leq S/D \leq 0.095$ can be divided into three phases from the observations.

Figure 6 shows the average, maximum, and minimum height of the visible flame tip for S/D ratios where a merging fire whirl was observed. These flame heights are the result of continuous measurement over 6 seconds in a steady state. The minimum and maximum values of the flame height are the continuous and intermittent flame heights, respectively. The continuous, intermittent and average flame heights decreased with increasing S/D. In the range of $S/D > 0.08$, the influence between adjacent flames was weak.

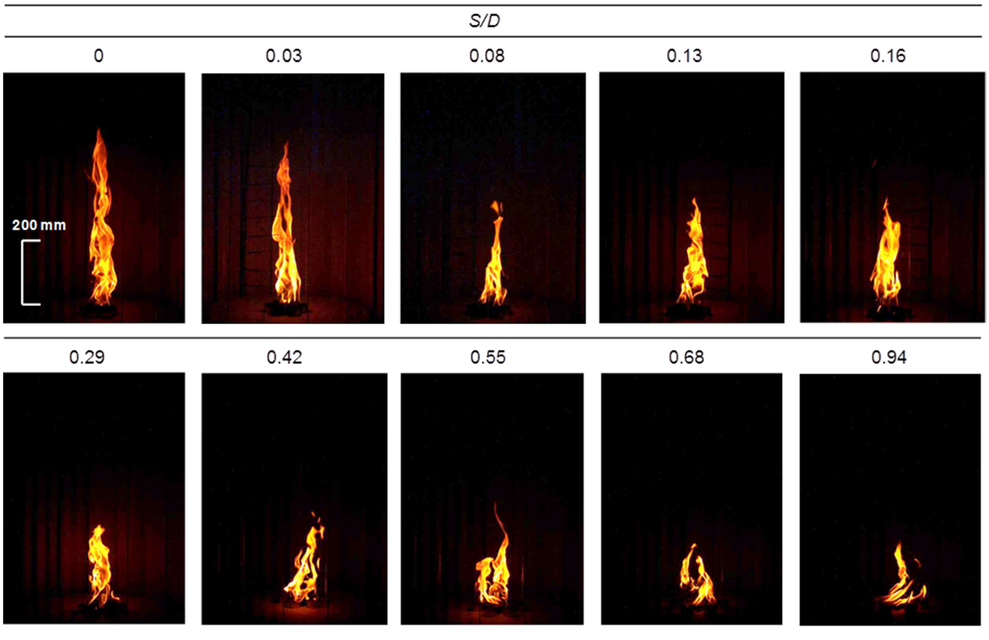

Fig. 5. Snapshots of flame structures during the steady state.

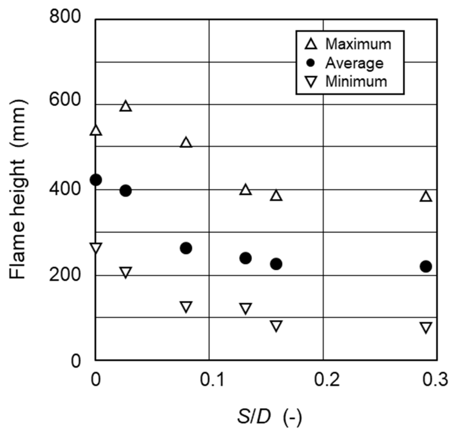

Fig. 6. Flame height change as a function of S/D.

Flame temperature

Figure 7 shows results for the relation between normalized vertical distance $z_t/\dot{q}^{2/5}$ and temperature rise ΔT along the central axis of the fire sources in the regions where a merging fire whirl was observed. This figure is organized based on the characteristic of temperature decay along the central axis of a flame driven by buoyancy. Figures 7 (a), (b), (c), and (d) show the cases where S/D = 0, 0.03, 0.08, and 0.13, respectively, when a merging fire whirl is observed. The intervals marked with letters at the top of each plot in Fig. 7 indicate the flame regions based on the results in Fig. 6. For purposes of comparison, the temperature attenuation in the flame center line obtained by the McCaffrey model is also shown in the figure. The solid line represents the McCaffrey results and the circles represent our results.

The values of ΔT in the continuous flame and intermittent flame regions increased compared to those of McCaffrey's model. In these flame regions, the decay rate of ΔT was almost the same as that of McCaffrey's model. In the plume region, ΔT was larger than that of the model. The increase of S/D only slightly changed the temperature of the continuous flame region, but this led to decreased intermittent flame and plume regions.

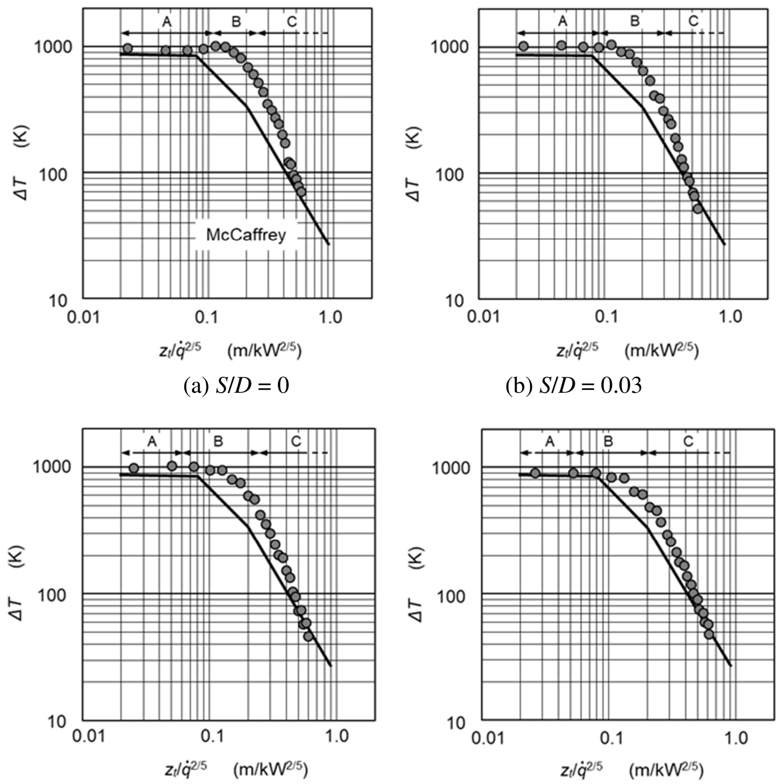

(a) S/D = 0 (b) S/D = 0.03

(c) S/D = 0.08 (d) S/D = 0.13

Fig. 7. Temperature attenuation along the central axis of fire source. A – continuous flame region; B – intermittent flame region; C – plume region.

Table 1 shows the ratio of the continuous flame and intermittent flame regions in the merging fire whirls, based on the range of continuous and intermittent flame regions for McCaffrey's model shown in Fig. 7. Because the values in Table 1 were calculated from the results in Fig. 6, they are linked with these regions, as indicated by arrows in Fig. 7. An increased S/D led to the contraction of the continuous flame region. In the case of S/D = 0 and 0.03, the continuous flame region expanded compared to that in McCaffrey's model. This result indicates that the strong and stable merging fire whirl expanded the continuous flame region. The intermittent flame region tended to expand when the continuous flame region contracted. These results indicate that the axial variations of temperature in the fire whirls of merged multiple flames did not conform to McCaffrey's model.

Table 1. Ratio of the continuous flame and intermittent flame regions

S/D (-)	Continuous flame region (-)	Intermittent flame region (-)
0	1.6	1.1
0.03	1.3	1.6
0.08	0.7	1.7
0.13	0.7	1.2
McCaffrey's model	1.0	1.0

Upward velocity of hot current

Figure 8 shows the variations in the upward velocity of the hot current along the central axis of fire sources in the regions where a strong and stable merging fire whirl was observed. Figures 8 (a), (b), (c), and (d) show the cases where S/D = 0, 0.03, 0.08, and 0.13, respectively. These figures are organized according to the upward velocity along the central axis of flame driven by buoyancy. The intervals marked with letters at the top of each plot indicate the flame regions based on the results in Fig. 6. For the purpose of comparison, the model for the upward velocity in the absence of crosswinds on the flame center line presented by McCaffrey is also shown in the figure.

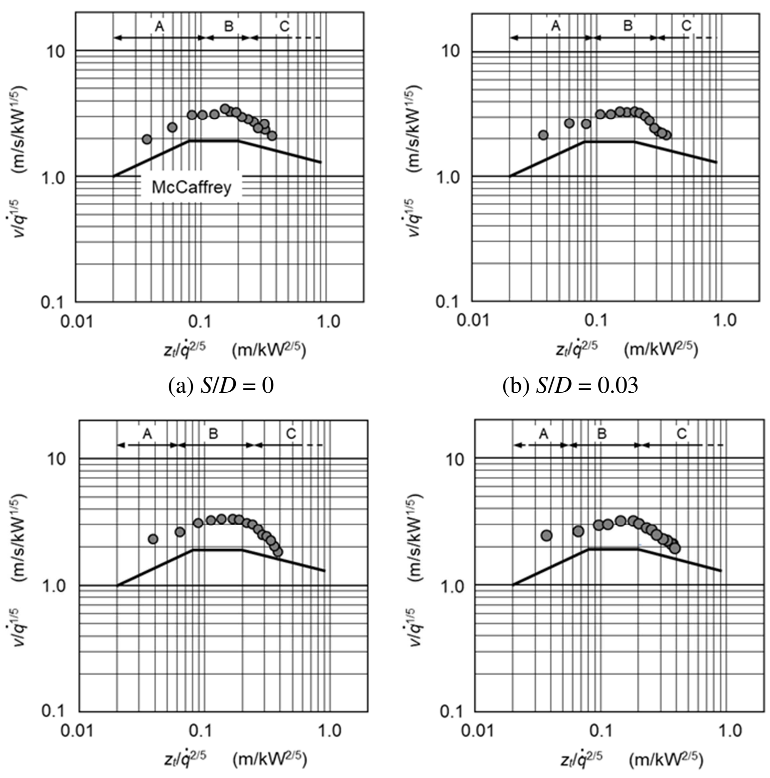

(a) $S/D = 0$ (b) $S/D = 0.03$

(c) $S/D = 0.08$ (d) $S/D = 0.13$

Fig. 8. Upward velocity of hot current along the central axis of fire source. A – continuous flame region; B – intermittent flame region; C – plume region.

The upward velocity of the hot current in the continuous flame, intermittent flame, and plume regions increased compared to those in McCaffrey's model, and they were hardly affected by increasing *S*/*D*. In the continuous and intermittent flame regions, the attenuation rate of the upward velocity was almost the same as that of the model. In the plume region, it was larger than that of the model. The axial variations of velocity of fire whirls formed from merged multiple flames did not conform to the model. Additionally, in this figure, although the result of the range of *S*/*D* where the merging fire whirl was not observed is omitted, the upward velocity was decreased relative to an increased *S*/*D*.

Velocity of airflow through air inlet

To examine the effect of entrained air on the burning process of the merging fire whirl, the velocity of the horizontal airflow through the air inlet was measured. Figure 9 shows the average velocities for *S*/*D* = 0, 0.03, and 0.08. This figure indicates an average velocity of crosswind through the air inlet in regions where the burning can be inferred to be in the steady state, as indicated by the heat release rate.

In the region where the merging flame is strong and stable, as shown in Fig. 9, the airflow velocity in the horizontal direction is strong at the base of the flame and becomes weak with increasing height over the base of the flame. Additionally, the dispersion of the velocity value for each *S*/*D* is low. Thus, the velocity of the horizontal airflow is generally independent of *S*/*D* in the region where the flames merge. This result indicates that *S*/*D* is dominant for changes in flame height of the merging fire whirl.

The entrained air gives not only the necessary impetus to maintain the swirling of the merging flame, but it also gives an inclination to the precession flames of the fire sources. When no guide plates were used, flame merger was observed at $0 \leq S/D \leq 0.08$ in our other experiments and the merging flame height increased with increasing *S*/*D*. The increase of *S*/*D* increases the difficulty of merging the precession flames; accordingly, the merging flame height attenuates.

Flame height of merging fire whirl

Figure 10 shows the relationship between fire source distance and dimensionless merging fire whirl height. The parameters L and L_m are average heights of the merging fire whirl in the case of $S/D = 0$ and $S/D > 0$, respectively. The solid curve in this figure is a fitting curve for the values of L/L_m.

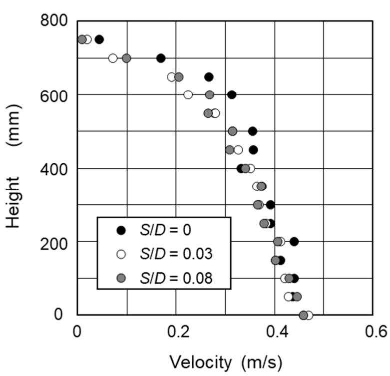

Fig. 9. Velocity of crosswind through the air inlet.

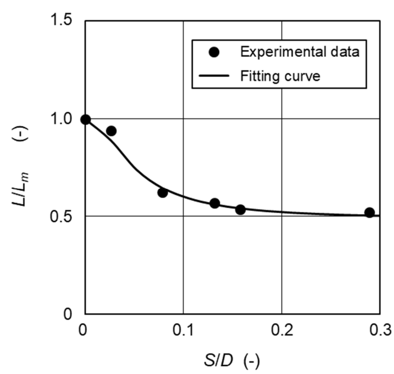

Fig. 10. Relationship between fire source distance and dimensionless merging fire whirl height.

Sugawa et al. proposed an experimental model to obtain the height of the flame tip when multiple circular pans are arranged near each other [15]. The equation for L/L_m is as follows:

$$L/L_m = ((nD^2 + S^2) / n (D^2 + S^2))^{2/5}, \quad (1)$$

where n is the number of fire sources. As a result of merging and swirling of multiple fire sources, when the merging fire whirl is formed, the flame tip becomes higher. Thus, because this model disregards flow other than upward airflow, there is a possibility that it cannot be applied to the estimation of the flame tip height of the merging fire whirl. We considered that the airflow velocities according to the magnitude of swirling flow from the outside influences the spatial term S (distance between fire sources). In addition, a hydrodynamic factor α on flow was newly added to the spatial term S of Sugawa's model equation, as shown in the following equation:

$$L/L_m = ((nD^2 + (\alpha_1 S)^2) / n (D^2 + (\alpha_2 S)^2)^{2/5}, \quad (2)$$

where α is a coefficient. In a fire source with free burning, α_1 and α_2 are 1; however, considering the influence of the fire whirlwind, α_1 acts in the direction in which the flame grows, and α_2 acts in the direction in which the flame contracts. Thus, the combined coefficient α is an indicator of the strength of the interaction between flames from different fire sources. It depends on the entrainment of the induced flow from the air inlet. When S/D is large, the interaction between the flames disappeared quickly as the induced flow from the air inlet flowed between fire sources.

When the value measured at S/D = 0.29 is used in Eq. (2), $L/L_m = (1/6)^{2/5}$ and this L/L_m can be interpreted as indicating the flame height for each pan. The fitting curve in Fig. 10 can be reproduced by Eq. (2), and this result indicates the possibility that Eq. (2) can be used to estimate the flame tip height of the merging fire whirl. When fitting the data to determine the value of α, α_1 = 24 and α_2 = 25 were adopted in the curve. The values of interaction strength coefficients α_1 and α_2 had no notable differences. To understand the details of coefficient α, we believe that it is necessary to clarify the behaviors of the airflow and flame corresponding to the relation between the angle of the air inlet, the number of fire sources, and the S/D ratio. Further exploration of the strength interaction coefficient is the subject of future work.

CONCLUSIONS

In this study, we experimentally investigated the variations in flame height behaviors for different spacings of fire sources in a tubular device with air inlets. The heat release rate, flame height, flame temperature, upward velocity, and airflow velocity were analyzed. The main conclusions are as follows:

1. The heat release rate decreased as S/D increased.
2. The range of $0 \leq S/D \leq 0.095$ is divided into a flame structure of three phases from the fire observations. In the range of $0 \leq S/D \leq 0.08$, the merging flame became strongly rotating and erect. In the range of $0.13 \leq S/D \leq 0.29$, a weak merging fire whirl with precession was observed. In the range of $0.42 \leq S/D \leq 0.95$, the multiple sources did not merge into a fire whirl.
3. A strong and stable merging fire whirl expanded the continuous flame region.
4. The axial variations of temperature and velocity of fire whirls formed from merged multiple flames did not conform to McCaffrey's model.
5. S/D is the dominant parameter for changing the flame height of the merging fire whirl. When S/D is increased, it is more difficult to merge the flame inclination caused by the entrained air from the air inlet; thus, the merging flame height attenuates.
6. Our results indicated that it might be possible to estimate the tip height of the merging fire whirl with our proposed model equation.

ACKNOWLEDGEMENTS

The authors gratefully thank Kazushi Ishida, Taisei Katsuno, and Yuki Tanaka of Sugawa Laboratory, Suwa University of Science, for their sincere contributions in conducting the tests.

REFERENCES

[1] R. Saxon, Atrium Buildings: Development and Design, The Architectural Press, London, 1986.

[2] L. Moosavi, N. Mahyuddin, N. Ghafar, Atrium Cooling Performance in a Low Energy Office Building in the Tropics, a Field Study, Build. Environ. 38 (2003) 409–426.

[3] R. Huo, W.K. Chow, X.H. Jin, Y.Z. Li, N.K. Fong, Experimental Studies on Natural Smoke Filling in Atrium due to a Shop Fire, Build. Environ. 40 (2005) 1185–1193.

[4] H.W. Emmons, S. Ying, The Fire Whirl, Proc. Combust Inst. 11 (1967) 475-488.

[5] A. Muraszew, J.B. Fedele, W.C. Kuby, The Fire Whirl Phenomenon, Combust. Flame 34 (1979) 29–45.

[6] K. Kuwana, S. Morishita, R. Dobashi, K.H. Chuah, K. Saito, The Burning Rate's Effect on the Flame Length of Weak Fire Whirls, Proc. Combust. Inst. 33 (2011) 2425–2432.

[7] H. Yua, S. Guoa, M. Penga, Q. Lia, J. Ruanb, W. Wana, C. Chena, Study on the Influence of Air-inlet Width on Fire Whirls Combustion Characteristic, Proceedings of the Asia-Oceania Symposium on Fire Science and Technology, Vol. 62 (2013) 813–820.

[8] R. Dobashi, T. Okura, R. Nagaoka, Y. Hayashi, T. Mogi, Experimental Study on Flame Height and Radiant Heat of Fire Whirls, Fire Technol. 52 (2016) 1069–1080.

[9] J. Lei, N. Liu, Flame Precession of Fire Whirls: A Further Experimental Study, Fire Saf. J. 79 (2016) 1–9.

[10] K.A. Hartl, A.J. Smits, Scaling of a Small Scale Burner Fire Whirl, Combust. Flame 163 (2016) 202–208.

[11] P. Wang, N. Liu, L. Zhang, Y. Bai, K. Satoh, Fire Whirl Experimental Facility with No Enclosure of Solid Walls: Design and Validation, Fire Technol. 51 (2015) 951–969.

[12] A.C.Y. Yuen, G.H. Yeoh, S.C.P. Cheung, Q.N. Chan, T.B.Y. Chen, W. Yang, H. Lu, Numerical study of the development and angular speed of a small-scale fire whirl, Comput. Sci. 27 (2018) 21–34.

[13] N. Liu, Q. Liu, J. S. Lozano, L. Zhang, Z. Deng, B. Yao, J. Zhu, K. Satoh, Multiple fire interactions: A further investigation by burning rate data of square fire arrays, Proc. Combust. Inst. 34 (2013) 2555–2564.

[14] P.H. Thomas, R. Baldwin, A.J.M. Heselden, Buoyant Diffusion Flames: Some Measurements of Air Entrainment, Heat Transfer, and Flame Merging, Proc. Combust. Inst. 10 (1965) 983–96.

[15] O. Sugawa, W. Takahashi, Flame Height Behavior from Multi-fire Sources, Fire Mater. (1993) 111–117.

[16] P.B. Dermer, A.Y. Varaksin, A.I. Leontiev, The Wall-free Non-stationary Fire Whirls Generation by Axisymmetric Burning of Solid Fuel Pellets, Heat Mass Transf. 110 (2017) 890–897.

[17] N. Watanabe, O. Sugawa, K. Kamiya, Influence of Air-inlet on Flame Merging Behavior for Multiple Fire Whirls, Proceedings of the Asia Pacific Symposium on Safety, SA2-03 (2017).

[18] J.G. McCaffrey, Purely Buoyant Diffusion Flames: Some Experimental Results, NBSIR79–1910, National Bureaus of Standard, Washington, DC, 1979.